Highly efficient, broadband coherent surface-mixing-wave generation using amplified surface plasmonic polaritons

C. J. Zhu, Y. Ren, X. Zhao, G. X. Huang, L. Deng, and E. W. Hagley

---

Articles you may be interested in

Highly efficient, broadband coherent surface-mixing-wave generation using amplified surface plasmonic polaritons

C. J. Zhu,[1,2] Y. Ren,[3] X. Zhao,[3] G. X. Huang,[2] L. Deng,[1] and E. W. Hagley[1]

[1]*National Institute of Standards and Technology, Gaithersburg, Maryland 20899, USA*
[2]*State Key Laboratory of Precision Spectroscopy and Department of Physics, East China Normal University, Shanghai 20006, China*
[3]*State Key Laboratory of Crystal Materials, Shandong University, Jinan 250100, China*

We show that coherent broadband surface mixing-wave (SMW) by a hyper-Raman process can be efficiently generated near a metallic surface abutting a quasi-three-level gain medium. The generation process is significantly enhanced by the amplified surface plasmonic polaritons (SPPs) in the gain layer, resulting in rapid growth of both fields. The highly efficient and directional amplified SPP and hyper-Raman SMW may facilitate engineering applications in which amplified-SPP propagation is desirable. © *2014 AIP Publishing LLC*. [http://dx.doi.org/10.1063/1.4878406]

Surface Plasmonic Polaritons (SPPs) are electric-charge-oscillation-based electromagnetic surface waves that exist at a dielectric-metal boundary.[1] These surface waves have been extensively investigated for many surface related phenomena such as sub-diffraction sensing,[2] surface imaging,[3] and subwavelength light guiding near the surface.[4–7] In addition, significantly high local SPP intensities near the surface can lead to strong enhancement of surface physical, chemical, and biological processes such as surface-enhanced Raman scattering (SERS),[8] optical sensing of nanoscale molecular complexes[9] down to single molecule[10] levels, SPP based lasing mechanisms,[11] and signal processing.[12]

Metallic surfaces, however, often have large intrinsic loss and this significantly limits practical SPPs-based applications.[1] To overcome this limitation, amplification of SPPs using a gain medium has received great attention.[13–20] Unfortunately, the efficiency of the gain provided by these methods is very low,[21,22] due to complications such as amplified spontaneous emission of SPPs.[23] Recently, amplification of SPPs using a three-level system similar to a flash-lamp pumped ruby laser has been proposed.[24,25] Kéna-Cohen *et al.* have shown SPPs amplification by side-pumping a segment of a metal surface coated with a gain layer.[26]

Coherent propagation growth is one of the most important features of highly efficient and highly directional mixing wave generation processes in nonlinear optics. Among its many practical advantages are significantly increased signal-to-noise ratios and drastically boosted signal strength which results in enhanced detectability of trace elements or chemical and biological agents. In this Letter, we exploit these features and investigate a highly efficient and highly directional broadband coherent surface mixing-wave (SMW) generation process[27] using an amplified SPP wave to provide the initial quantum Raman coherence. In this surface enhanced parametric amplification process, the SPP generated by a separate pump provides the initial coherent seed field and it is subsequently amplified together with the SMW by a single pump field in the gain medium (Fig. 1). The major feature of our work, however, is the propagation amplification effects of the SPPs and seeded surface hyper-Raman/mixing-wave that are not included in the SPP amplification studies reported in Refs.

24–26, 28, and 29. Indeed, both Refs. 28 and 29 reported localized surface four-wave mixing (FWM) without any coherent propagation effect. We show by extensive numerical simulations that such coherent surface propagation effects can lead to significant surface wave amplification and growth characteristics similar to parametric processes on the surface of a nonlinear sheet produced by ion implantation.[27,30]

Consider a plane-polarized electromagnetic wave $\mathbf{E}_0(\omega_0)$ incident on a gold nano-film from below at a frequency-dependent "resonance angle" $\theta_r(\omega_0)$ (Fig. 1) that effectively excites SPPs modes of frequency $\omega_{\mathrm{SPPs}} \approx \omega_0$ on the surface of the gold nano-film. Above the gold nano-film is a layer of a three-level gain medium that is illuminated by a strong pump field $\mathbf{E}_L$ traveling parallel to the surface of the gold nano-film.[31] The pump field couples the $|g\rangle \rightarrow |e\rangle$ via a multi-photon process with a multi-photon detuning of δ_e (Fig. 1), resulting in a spontaneous emission of a SMW field E_{SMW} from state $|e\rangle \rightarrow |m\rangle$. The evanescent tail of SPPs excited by $\mathbf{E}_0$ extends well into the gain medium, behaving as a broadband coherent seed wave that couples the $|m\rangle \leftrightarrow |g\rangle$ transition of three-level system constituting the gain medium. This seeding action transforms the characteristics of the
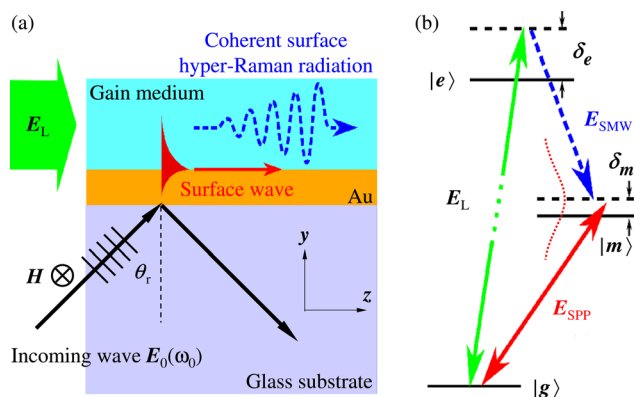
FIG. 1. (a) Schematic of the coherent SMW generation assisted by amplification of SPPs near a dielectric-metallic interface. (b) Energy levels of the three-level gain medium. The $|g\rangle \leftrightarrow |e\rangle$ transition is driven by a multi-photon pump field. The SPPs field (dashed curve indicates SPP bandwidth) couples the $|g\rangle \leftrightarrow |m\rangle$ transition whereas the SMW field is generated via the $|e\rangle \rightarrow |m\rangle$ transition.

mixing-wave emission from spontaneous to "*coherently lock-ed*" to the SPP wave as the two surface waves propagate, resulting in a highly directional, coherently amplified process. Indeed, early absorption of the SPP field by the gain medium establishes a Raman coherence, resulting in coherent and highly directional SMW that further amplifies the SPP wave.

The above described physical picture can be obtained by solving the Maxwell Equation of the SPP field $\mathbf{E}_{\mathrm{SPPs}}$ with appropriate boundary conditions[1] and the effective permittivity of the material ϵ_α where $\alpha = (s, M, b)$ denotes the substrate, metal, and gain layers, respectively. The complex permittivity of metal is obtained from the Drude-Lorentz model[32]

$$\epsilon_M = \epsilon_\infty - \frac{\omega_{\mathrm{D}}^2}{\omega(\omega + i\gamma_{\mathrm{D}})} - \frac{\Delta\epsilon\,\Omega_{\mathrm{L}}^2}{(\omega^2 - \Omega_{\mathrm{L}}^2) + i\Gamma_{\mathrm{L}}\omega}, \quad (1)$$

where $\omega = \omega_0$ is the center angular frequency of the incoming field, $\epsilon_\infty = 5.9675$. The Drude model plasma frequency and attenuation constant are $\omega_{\mathrm{D}}/2\pi = 2113.6\,\mathrm{THz}$ and $\gamma_{\mathrm{D}}/2\pi = 15.92\,\mathrm{THz}$, respectively, and $\Delta\epsilon = 1.09$ for an Au film. The Drude-Lorentz model parameters are $\Omega_{\mathrm{L}}/2\pi = 650.07\,\mathrm{THz}$ and $\Gamma_{\mathrm{L}}/2\pi = 104.86\,\mathrm{THz}$, respectively, representing the interband transition strength and Lorentz line shape of such a transition.

Without the gain medium pump field $\mathbf{E}_{\mathrm{L}}$, the permittivity of the gain medium ϵ_b can be described effectively using a two-level model involving states $|m\rangle$ and $|g\rangle$ is given by $\epsilon_b = 1 + \kappa_{mg}/[\delta_m + i\gamma_m]$, where $\kappa_{mg} = \mathcal{N}_a|\mathbf{p}_{mg}|^2/(\epsilon_0\hbar)$ with $\mathcal{N}_a$ being the density of the three-state atoms in the gain medium and $\mathbf{p}_{mg}$ being the electric-dipole moment between states $|m\rangle$ and $|g\rangle$. γ_m and δ_m are the resonance line width and detuning of the SPPs field from the state $|m\rangle$, respectively. In Fig. 2(a), we show the real and imaginary parts of the effective index change $\delta n_b = \epsilon_b - 1$ of the gain medium as a function of frequency using an atom density $\mathcal{N}_a = 10^{12}/\mathrm{cm}^3$ and $\gamma_m/2\pi = 3\,\mathrm{GHz}$. Here, the blue dashed curve indicates a significant increase in the attenuation constant at the SPPs field center frequency in the gain medium when the pump field $\mathbf{E}_{\mathrm{L}}$ is absent. Figure 2(b) shows the SPPs field mode size $D_{\mathrm{SPPs}} = \lambda_0/[2\pi\sqrt{(\mathrm{Re}[n_{\mathrm{SPPs}}])^2 - 1}]$ (dashed line) and propagation length $L_{\mathrm{SPPs}} = \lambda_0/2\pi\mathrm{Im}[n_{\mathrm{SPPs}}]$ (solid line) in the absence of $\mathbf{E}_{\mathrm{L}}$ as a function of SPP pump wavelength λ_0 where the complex effective index of the SPPs field $n_{\mathrm{SPPs}} = \sqrt{\epsilon_b\,\epsilon_M/(\epsilon_b + \epsilon_M)}$. We note that the choice of the large relaxation rate γ_m in our calculation is to account for environment-broadening effects such as the Purcell enhancement factor to the spontaneous emission rate of an atomic emitter near a metal surface, which typically has a spontaneous emission rate of 10 MHz.

The evolution of the SMW field and the SPP field can be calculated using coupled Maxwell equations

$$\nabla^2 E_\beta + k_\beta^2 E_\beta = k_\beta^2 P_\beta/\epsilon_0, \quad (\beta = \mathrm{SMW\ or\ SPPs}), \quad (2)$$

where $P_{\mathrm{SMW}} = \mathcal{N}_a|\mathbf{p}_{em}|A_eA_m^*$ and $P_{\mathrm{SPPs}} = \mathcal{N}_a|\mathbf{p}_{mg}|A_mA_g^*$ and $A_j\ (j = g,m,e)$ are the material wavefunction amplitudes.

Under the electric-dipole and rotating-wave approximations the system Hamiltonian in the interaction picture is

$$\hat{H} = \delta_e|e\rangle\langle e| + \delta_m|m\rangle\langle m| - [\mathbf{p}_{mg} \cdot \mathbf{E}_{\mathrm{SPPs}}|m\rangle\langle g|$$
$$+ \mathbf{p}_{em} \cdot \mathbf{E}_{\mathrm{SMW}}|e\rangle\langle m| + \mathbf{p}_{eg} \cdot \mathbf{E}_{\mathrm{L}}|e\rangle\langle g| + \mathrm{c.c.}], \quad (3)$$

and the atomic-response equations of motion are given by

$$i\frac{\partial}{\partial t}A_m + d_mA_m + \Omega_{\mathrm{SMW}}^*A_e + \Omega_{\mathrm{SPPs}}A_g = 0, \quad (4a)$$

$$i\frac{\partial}{\partial t}A_e + d_eA_e + \Omega_LA_g + \Omega_{\mathrm{SMW}}A_m = 0, \quad (4b)$$

subject to the total population conservation condition $|A_g|^2 + |A_m|^2 + |A_e|^2 = 1$. Here, $A_j\ (j = g, m, e)$ is the amplitude of the atomic state $|j\rangle$, $d_j = \delta_j + i\gamma_j$ with δ_j and γ_j being the detuning and total decay rate of state $|j\rangle$. $\Omega_{\mathrm{L,SMW,SPPs}} \equiv \mathbf{p}_{eg,em,gm} \cdot \mathbf{E}_{\mathrm{L,SMW,SPPs}}/\hbar$ are the half-Rabi frequencies of the effective multiphoton pump, SMW, and SPPs fields.

We numerically solve Eqs. (2), (4a), and (4b) using a 20-μm thick layer of three-level atomic gain medium on a $1\,\mathrm{cm} \times 1\,\mathrm{cm}$ chip having a 50 nm Au nanolayer on a glass substrate. In the absence of the hyper-Raman pump field $\mathbf{E}_{\mathrm{L}}$, no hyper-Raman SMW field is generated inside the gain layer and the SPP wave is strongly attenuated [Fig. 3(a)].
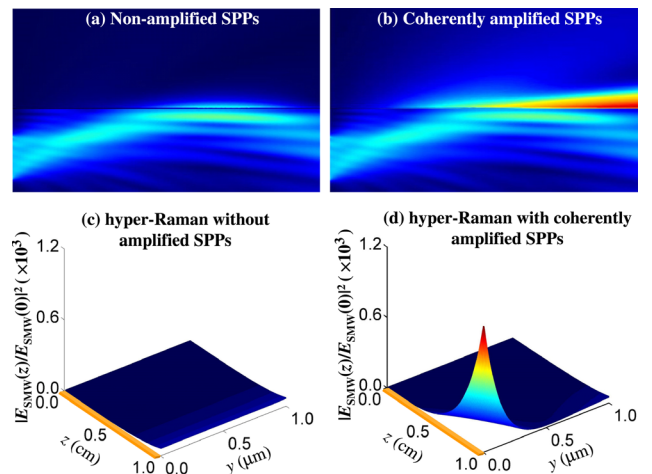
FIG. 3. Numerical calculation of the SPP field in an atomic gain medium without (a) and with (b) the pump field $\mathbf{E}_{\mathrm{L}}$ and $\mathbf{E}_{\mathrm{SMW}}$. Coherent SMW generation without (c) and with (d) the amplified-SPPs in a layer of gaseous phase atomic gain medium. Parameters: $\gamma_e/2\pi = 6\,\mathrm{GHz}$, $\gamma_m/2\pi = 3\,\mathrm{GHz}$, $\delta_e/2\pi = 10\,\mathrm{GHz}$, $\delta_m/2\pi = 1\,\mathrm{GHz}$, density $10^{12}/\mathrm{cm}^3$, and $\Omega_L/2\pi = 3\,\mathrm{GHz}$. SPP pump $\lambda_0 = 700\,\mathrm{nm}$.
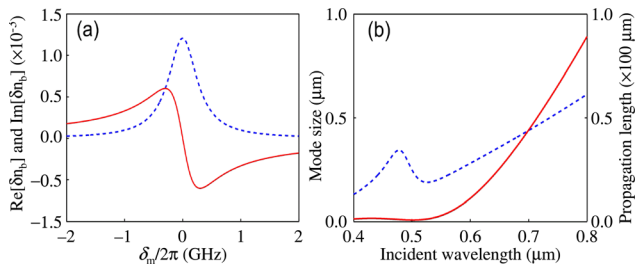

FIG. 2. (a) Real (solid line) and imaginary (dashed line) parts of the index change $\delta n_b = \epsilon_b - 1$ of the gain medium as a function of the SPP field detuning in a two-level model. (b) SPP field mode size (dashed line) and propagation length (solid line) as a function of the pump wavelength in the absence of $\mathbf{E}_{\mathrm{L}}$) in the gain medium. Parameters: $\gamma_e/2\pi = 6\,\mathrm{GHz}$, $\gamma_m/2\pi = 3\,\mathrm{GHz}$, $\delta_e/2\pi = 10\,\mathrm{GHz}$, and $\Omega_L = 0\,\mathrm{Hz}$.

Correspondingly, no hyper-Raman SMW field can be efficiently generated as well [Fig. 3(c)].

To overcome the SPP field attenuation, we now introduce an external multi-photon pump field $\mathbf{E}_L$ that propagates along the direction of the effective $\mathbf{k}_{SPP}$ (Fig. 1). This pump field excites the multi-photon transition $|g\rangle \leftrightarrow |e\rangle$ with an effective detuning δ_e, resulting in an active gain medium that coherently generates a hyper-Raman SMW via the transition $|e\rangle \rightarrow |m\rangle$ and also contributes to the amplification of the SPP field. Figure 3(b) shows the SPP wave amplification under the action of coherent propagation gain enabled by the hyper-Raman pump field $\mathbf{E}_L$. Accompanying this coherent amplification of the SPP field is the rapid growth of a highly directional hyper-Raman SMW field [Fig. 3(d)]. In essence, by coupling the states $|g\rangle$ and $|m\rangle$, the SPP field provides a coherent seed wave that modifies the Raman coherence which, under the action of the external pump field $\mathbf{E}_L$, results in simultaneous coherent generation and amplification of both the SMW and SPP fields.

It is worth pointing out that the SPP-assisted SMW field generation has mixed characteristics of parametric FWM and hyper-Raman radiation. The former is due to the broad phase matching regions supported by the broad bandwidth of SPPs, whereas the latter is dominantly an on resonance process. Both of these characteristics have been observed in alkali metal vapor experiments[33] using configurations similar to that shown in Fig. 1(b).

One of the key features of an atomic Raman gain medium is the long lifetime of the atomic Raman state. Such a narrow Raman resonance significantly enhances the coherent propagation effect and therefore dramatically increases the signal-to-noise ratio which can lead to a significant reduction in data acquisition time.[34] In most solid state and soft condensed matter materials, however, the molecular Raman states usually have a much broader Raman resonance linewidth. For instance, a typical molecular vibrational Raman terminal state often has a linewidth of few wave numbers and this significantly impacts the propagation gain coefficient. Nevertheless, we show below that significant enhancement of hyper-Raman SMW and amplification of SPPs can still be achievable for many molecular Raman radiators.

To illustrate the potential of the coherent-wave-enhancement effect for SPP amplification using molecular Raman gain medium and to further explore possible advantages of combining the coherent wave propagation effect with the local surface field enhancement effect, we consider a case with a generic molecular gain medium with density $\mathcal{N}_a = 10^{14}/cm^3$. This density is about two orders of magnitude less than the typical laser dye lasing concentration,[35] indicating the viability of the SPP-SMW amplification scheme described in this work. The molecule gain layer is 20 μm in thickness and the hyper-Raman state $|m\rangle$ has a relaxation rate of $\gamma_m/2\pi = 100\,GHz$. Figures 4(a) and 4(b) show the SPP amplification without and with the hyper-Raman pump field. Here, the SPP pump field illuminates the Au layer from underneath through the glass substrate as in Fig. 3 but we add a nano-grating segment[36,37] (grating groves are 100 nm in height, 150 nm in width, and have a 150 nm separation) to the left-end of the Au nano-layer and use a separate pump laser to excite the grating vertically.[38] Numerical
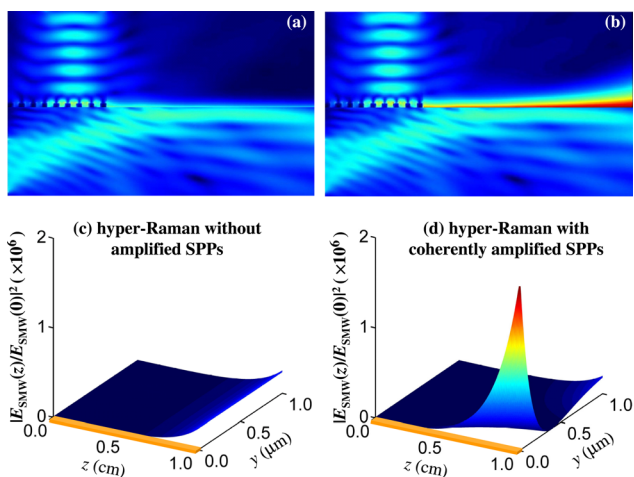

FIG. 4. Numerical calculation of the SPP field in a molecular gain medium without (a) and with (b) the hyper-Raman pump field $\mathbf{E}_L$. Here, a nano-grating segment is added to the left end of the surface and a separate pump field illuminates the nano-grating vertically. Coherent hyper-Raman SMW propagation growth without (c) and with (d) the amplified-SPP. Parameters: $\gamma_e/2\pi = 100\,GHz$, $\gamma_m/2\pi = 100\,GHz$, $\delta_e/2\pi = 1000\,GHz$, $\delta_m/2\pi = 80\,GHz$, density $10^{14}/cm^3$, and . SPP pump $\lambda_0 = 700\,nm$.

calculations show that this combination of a vertically excited nano-grating and obliquely excited Au layer results in more efficient generation of the amplified-SPPs and hyper-Raman SMW.

The coherent SPP-amplification enhanced hyper-Raman field growth in the molecular gain layer in this combination structure is shown in Figs. 4(c) and 4(d) for the case of without and with the coherently amplified SPP. We also find that the nano-grating segment added increases the hyper-Raman SMW by more than 20%. These results again show the significant propagation growth of the hyper-Raman field that is further enhanced by the coherent growth of the amplified SPP field.

In conclusion, we have investigated coherent amplification and propagation growth of SPPs near the interface of a metal film and a dielectric gain medium in the presence of SMW originating from hyper-Raman growth in the gain medium. Without an external Raman pump, the SPP decays rapidly in the gain layer and coherent propagation growth is not supported. With an external Raman pump in the gain layer, however, significant amplification of the SPP occurs. The amplified SPP grows and further enhances the Raman coherence of the gain medium, strongly supporting a highly directional, highly efficient generation of a hyper-Raman SMW. The study reported here may provide an effective scheme for engineering applications of surface plasmonic polaritons.

[1]V. M. Agranovich and D. L. Mills, *Surface Polaritons: Electromagnetic Waves at Surfaces and Interfaces* (North-Holland, Amsterdam, 1982).
[2]S. A. Maier, P. G. Kik, H. A. Atwater, S. Meltzer, E. Harel, B. E. Koel, and A. A. G. Requicha, Nature Mater. **2**, 229 (2003).
[3]I. I. Smolyaninov, J. Elliott, A. V. Zayats, and C. C. Davis, Phys. Rev. Lett. **94**, 057401 (2005).

[4]S. I. Bozhevolnyi, V. S. Volkov, and K. Leosson, Phys. Rev. Lett. **89**, 186801 (2002).

[5]S. E. Bozhevolnyi, V. S. Volkov, E. Devaux, J. Y. Laluet, and T. W. Ebbesen, Nature **440**, 508 (2006).

[6]W. L. Barnes, A. Dereux, and T. W. Ebbesen, Nature **424**, 824 (2003).

[7]M. I. Stockman, Phys. Rev. Lett. **93**, 137404 (2004).

[8]*Surface-Enhanced Raman Scattering: Physics and Applications*, edited by K. Kneipp, M. Moskovits, and H. Kneipp (Springer, Berlin Heidelberg, 2006).

[9]D. V. Voronine, A. M. Sinyukov, X. Hua, K. Wang, P. K. Jha, E. Munusamy, S. E. Wheeler, G. Welch, A. V. Sokolov, and M. O. Scully, Sci. Rep. **2**, 891 (2012).

[10]B. Sharma, R. R. Frontiera, A. Henry, E. Ringe, and R. P. V. Duyne, Mater. Today **15**, 16 (2012).

[11]P. Berini and I. D. Leon, Nat. Photonics **6**, 16 (2012).

[12]M. I. Stockman, Opt. Express **19**, 22029 (2011).

[13]D. J. Bergman and M. I. Stockman, Phys. Rev. Lett. **90**, 027402 (2003).

[14]J. Seidel, S. Grafstroem, and L. Eng, Phys. Rev. Lett. **94**, 177401 (2005).

[15]M. A. Noginov, G. Zhu, A. M. Belgrave, R. Bakker, V. M. Shalaev, E. E. Narimanov, S. Stout, E. Herz, T. Suteewong, and U. Wiesner, Nature (London) **460**, 1110 (2009).

[16]R. F. Oulton, V. J. Sorger, T. Zentgraf, R.-M. Ma, C. Gladden, L. Dai, G. Bartal, and X. Zhang, Nature (London) **461**, 629 (2009).

[17]J. Grandidier, G. Francs, S. Massenot, A. Bouhelier, L. Markey, J. C. Weeber, C. Finot, and A. Dereux, Nano Lett. **9**, 2935 (2009).

[18]D. Y. Fedyanin, A. V. Krasavin, A. V. Arsenin, and A. V. Zayats, Nano Lett. **12**, 2459 (2012).

[19]K. Leosson, J. Nanophotonics **6**, 061801 (2012).

[20]D. Y. Fedyanin and A. V. Arsenin, Opt. Express **19**, 12524 (2011).

[21]J. B. Khurgin and G. Sun, Appl. Phys. Lett. **100**, 011105 (2012).

[22]J. B. Khurgin and G. Sun, Nanophotonics **1**, 3 (2012).

[23]P. M. Bolger, W. Dickson, A. V. Krasavin, L. Liebscher, S. G. Hickey, D. V. Skryabin, and A. V. Zayats, Opt. Lett. **35**, 1197 (2010).

[24]P. K. Jha, X. Yin, and X. Zhang, Appl. Phys. Lett. **102**, 091111 (2013).

[25]K. E. Dorfman, P. K. Jha, D. V. Voronine, P. Genevet, F. Capasso, and M. O. Scully, Phys. Rev. Lett. **111**, 043601 (2013).

[26]S. Kéna-Cohen, P. N. Stavrinou, D. D. C. Bradley, and S. Maier, Nano Lett. **13**, 1323–1329 (2013).

[27]Y. R. Shen, Nature **337**, 519 (1989).

[28]S. Palomba and L. Novotny, Phys. Rev. Lett. **101**, 056802 (2008).

[29]J. Renger, R. Quidant, N. van Hulst, and L. Novotny, Phys. Rev. Lett. **104**, 046803 (2010).

[30]*Engineering Thin Films and Nanostructures with Ion Beam*, edited by É. Knystautas (Taylor & Francis Group, 2005).

[31]Because of the significant difference in wavelength SPPs produced by E_L due to beam divergence are outside the frequency region considered and will not affect the performance of the gain medium.

[32]A. Vial, A.-S. Grimault, D. Macias, D. Barchiesi, and M. L. de la Chapelle, Phys. Rev. B **71**, 085416 (2005).

[33]W. R. Garrett, M. A. Moore, R. C. Hart, M. G. Payne, and R. Wunderlich, Phys. Rev. A **45**, 6687 (1992).

[34]In microscope-based surface-enhanced Raman scattering protocols, the laser beam must be very tightly focused ($\sim\mu$m) in order to obtain a significant enhancement to the spontaneous Raman scattering. Such a small interaction region requires a significantly long data acquisition cycle to extract useful signal across the sample chip.

[35]*Dye Lasers*, edited by F. P. Miller, A. F. Vandome, and J. McBrewster (VDM Publishing House, Ltd., 2010).

[36]K. H. Yoon, M. L. Shuler, and S. J. Kim, Opt. Express **14**, 4842 (2006).

[37]A. Dhawan, M. Canva, and T. Vo-Dihn, Opt. Express **19**, 787 (2011).

[38]The parallel beam grating pump cannot efficiently couple into the Au layer because of the wave vector mismatch.